Journal of Mathematical Biology (2023) 86:21
https://doi.org/10.1007/s00285-022-01855-8

Mathematical Biology

An age-dependent immuno-epidemiological model with distributed recovery and death rates

Samiran Ghosh[1] · Vitaly Volpert[2,3] · Malay Banerjee[1]

Received: 24 August 2022 / Revised: 6 December 2022 / Accepted: 9 December 2022 /
Published online: 10 January 2023

Abstract

The work is devoted to a new immuno-epidemiological model with distributed recovery and death rates considered as functions of time after the infection onset. Disease transmission rate depends on the intra-subject viral load determined from the immunological submodel. The age-dependent model includes the viral load, recovery and death rates as functions of age considered as a continuous variable. Equations for susceptible, infected, recovered and dead compartments are expressed in terms of the number of newly infected cases. The analysis of the model includes the proof of the existence and uniqueness of solution. Furthermore, it is shown how the model can be reduced to age-dependent SIR or delay model under certain assumptions on recovery and death distributions. Basic reproduction number and final size of epidemic are determined for the reduced models. The model is validated with a COVID-19 case data. Modelling results show that proportion of young age groups can influence the epidemic progression since disease transmission rate for them is higher than for other age groups.

Keywords Immuno-epidemiological model · Distributed recovery and death rates · Age structure · Existence of solution · COVID-19

Mathematics Subject Classification 34K60 · 92D30

✉ Malay Banerjee
malayb@iitk.ac.in

Samiran Ghosh
samiran@iitk.ac.in

Vitaly Volpert
volpert@math.univ-lyon1.fr

1 Department of Mathematics and Statistics, Indian Institute of Technology Kanpur, Kanpur 208016, Uttar Pradesh, India

2 Institut Camille Jordan, UMR 5208 CNRS, University Lyon 1, 69622 Villeurbanne, France

3 Peoples Friendship University of Russia (RUDN University), 6 Miklukho-Maklaya St, 117198 Moscow, Russian Federation

1 Introduction

Major epidemic outbreaks such as H5N1 influenza in 2005 (Chen et al. 2006; Kilpatrick et al. 2006), H1N1 in 2009 (Girard et al. 2010), Ebola in 2014 (Frieden et al. 2014) and very recently COVID-19 pandemic have strong influence on public health and world economy. Mathematical models in epidemiology, starting with fundamental works by Daniel Bernoulli in XVIII century and by W.O. Kermack and A.G. McKendrick in the beginning of the last century (Kermack and McKendrick 1927, 1932, 1933) allow the description of epidemic progression and elaboration of proper control measures. More recent developments in mathematical epidemiology include multi-compartmental models (Brauer 2008; Brauer et al. 2019; Chattopadhyay et al. 2021), models with nonlinear transmission rate (Fenichel et al. 2011; Hethcote and Van den Driessche 1991), multi-patch models (Bichara and Iggidr 2018; Gao and Ruan 2012; Jansen and Lloyd 2000), agent-based models (Bouchnita and Jebrane 2020; Rockett et al. 2020), network models (Bansal et al. 2007; Lindquist et al. 2011), multi-scale models (Barbarroux et al. 2016, 2018), immuno-epidemic models (Bocharov et al. 2018; Ghosh et al. 2022b; Gilchrist and Sasaki 2002).

Compartmental epidemiological models, such as conventional SIR model, are based on the assumption that the rate of disease transmission is proportional to the product of the number of susceptible $S(t)$ and infected $I(t)$ individuals at time t. Another important assumption is that the recovery and death rates at time t are proportional to the number of infected $I(t)$ at the same moment of time. It neglects disease duration and can lead to a significant discrepancy. Indeed, if an average disease duration is τ, then the number of recoveries and deaths at time t is determined by $I(t-\tau)$ and not by $I(t)$. During the periods of exponential growth or decay of the number of infected individuals, the difference between them can be quite essential.

In order to get a more precise description of epidemic progression, the recovery and death rates should be considered as distributed functions of the time-since-infection. Moreover, the within-body viral dynamics and recovery time are patient-specific and depend, in particular, on age group (Vattiatio et al. 2022). Hence, more detailed epidemiological models should take into account the heterogeneity of the population. Among different types of population heterogeneity, age-structure is one of the most crucial factors in disease progression. As example, although malaria affects people of all age groups, children have the highest risk of infection. The incidence of HIV is highest in the age group 20-45 years. The death rate of the recent coronavirus disease also strongly depends on the age group (Levin et al. 2020).

Linear age-structured epidemic models were considered in von Foerster (1959). More recent developments include nonlinear models (Liu et al. 2018), age-structured model with diffusion (Kang and Ruan 2021; Ou and Wu 2006) and vaccination (Castillo-Chavez and Feng 1998; Müller 1998; Shim et al. 2006), with age-since-infection (Li et al. 2020; Qesmi et al. 2011, 2015), periodic infection rate (Kang et al. 2020; Kuniya and Inaba 2013), multi-group age-structured model (Kuniya 2011; Kuniya et al. 2016). Age-since-infection is used in immuno-epidemiological models where the within-host dynamics is linked to the between-host dynamics. For simplicity, it is often assumed that the within-host dynamics is the same for all individuals, though this approximation may not be justified for every epidemic diseases.

In this work we propose a new immuno-epidemiological model with time-distributed and age-dependent recovery and death rates. In some particular cases, this model can be reduced to age-dependent SIR and delay models.

The contents of the paper are as follows. In Sect. 2 we introduce an age-dependent immunological model and determine viral load which will determine the infectivity rate in the epidemiological model. In Sect. 3, we propose an age-dependent immuno-epidemiological model with distributed recovery and death rates. Existence and uniqueness of solution are proved. Next, we reduce this model to an age-dependent SIR model and calculate some relevant epidemiological quantities in Sect. 4. In Sect. 5, we discuss the properties of a delay model which can be derived for a particular choice of the recovery and death distributions. In Sect. 6, we estimate model parameters. Some numerical results and the model validation with the data on Omicron variant of SARS-CoV-2 infection are discussed in Sect. 7.

2 Immunological submodel

In this section we determine viral load in infected individuals. It will be used below in the epidemiological model in order to determine the infectivity rate. Consider the following model for infection development in the human organism:

$$\frac{du}{dt} = -auv, \tag{2.1a}$$

$$\frac{dz}{dt} = auv - \sigma_1 z, \tag{2.1b}$$

$$\frac{dv}{dt} = bz(t-\theta) - \sigma_2 v, \tag{2.1c}$$

where u is the concentration of uninfected cells in the target tissue, z is the concentration of infected cells, and v is the concentration of virus within an individual at time t; θ is time delay in virus replication (Baccam et al. 2006). Parameter a characterizes the infection rate of uninfected target cells, σ_1 is the death rate of infected cells, σ_2 is the clearance rate of virus, b is the virus production rate in infected cells. The model (2.1) is subject to the initial conditions:

$$u(0) = u_0, \quad v(0) = v_0, \quad z(t) = 0, \quad -\theta \le t \le 0. \tag{2.2}$$

Here v_0 is the initial viral load. Parameters of this model and its solution can depend on patient's age. In particular, innate and adaptive immune responses, which are taken implicitly into account in the coefficients σ_1 and σ_2 are patient-specific and depend on the age group.

2.1 Virus replication number

The disease-free equilibrium for model (2.1) is $(u_0, 0, 0)$. The corresponding characteristic equation is as follows:

$$\lambda\left(\lambda^2 + (\sigma_1 + \sigma_2)\lambda + \left(\sigma_1\sigma_2 - abu_0e^{-\lambda\theta}\right)\right) = 0.$$

Let us set

$$f(\lambda) \equiv \lambda^2 + (\sigma_1 + \sigma_2)\lambda + (\sigma_1\sigma_2 - abu_0e^{-\lambda\theta}).$$

Then

$$f(0) = \sigma_1\sigma_2 - abu_0 = \sigma_1\sigma_2\left(1 - \frac{abu_0}{\sigma_1\sigma_2}\right),$$

and for all real $\lambda > 0$,

$$f'(\lambda) = 2\lambda + \sigma_1 + \sigma_2 + abu_0\theta e^{-\lambda\theta} > 0.$$

Also note that $\lim_{\lambda\to\infty} f(\lambda) = \infty$. Since $f'(\lambda) > 0$ for all $\lambda > 0$, it can be easily observed that equation $f(\lambda) = 0$ has a positive root if $\frac{abu_0}{\sigma_1\sigma_2} > 1$. There are no positive roots if the inequality is opposite.

Let us introduce the virus replication number for the immunological model (2.1):

$$\mathcal{R}_v = \frac{abu_0}{\sigma_1\sigma_2}. \tag{2.3}$$

If $\mathcal{R}_v > 1$, then virus concentration grows in the beginning of the infection progression, then it reaches maximum and converges to 0 due to the exhaustion of infected cells. If the virus replication number is less than 1, infection does not develop.

In the next section we will introduce the total viral load and will determine it with the help of the virus replication number.

2.2 Total viral load

Let us note that $z(\infty) = v(\infty) = 0$ and use the notation $u_f = u(\infty)$. Then from equation (2.1a) we obtain:

$$\ln\left(\frac{u_f}{u_0}\right) = -a\int_0^\infty v(t)dt. \tag{2.4}$$

Taking a sum of equations (2.1a) and (2.1b) and integrating over the time interval $[0, \infty)$, we obtain:

$$u_f - u_0 = -\sigma_1 \int_0^\infty z(t)dt. \tag{2.5}$$

Finally, integrating equation (2.1c), we get:

$$-v_0 = b\int_0^\infty z(t)dt - \sigma_2 \int_0^\infty v(t)dt. \tag{2.6}$$

Define the total viral load as the integral of virus concentration with respect to time:

$$W = \int_0^\infty v(t)dt.$$

Then we get from equations (2.4) and (2.5):

$$\int_0^\infty z(t)dt = (u_0 - u_f)/\sigma_1 = \frac{u_0}{\sigma_1}\left(1 - e^{-aW}\right).$$

Hence, from (2.6),

$$W - \frac{v_0}{\sigma_2} = \frac{u_0 b}{\sigma_1 \sigma_2}\left(1 - e^{-aW}\right). \tag{2.7}$$

Introducing the notation $\overline{W} = aW$, $\overline{w}_0 = av_0/\sigma_2$, we can write the last equation as follows:

$$\overline{W} - \overline{w}_0 = \mathcal{R}_v\left(1 - e^{-\overline{W}}\right), \tag{2.8}$$

where $\mathcal{R}_v$ is defined in (2.3). If we suppose that the initial viral load is small enough, that is $\overline{w}_0 \approx 0$, then equation (2.8) becomes:

$$\overline{W} = \mathcal{R}_v\left(1 - e^{-\overline{W}}\right). \tag{2.9}$$

This equation has a positive solution $\overline{W}$ if and only if $\mathcal{R}_v > 1$. If the parameters of the model (2.1) depend on patient's age x, then we obtain an age-dependent viral load $W(x) = \int_0^\infty v(x,t)dt$ which determines the disease transmission rate (D'Agata et al. 2006; Webb et al. 2005).

3 Age-dependent immuno-epidemic model with time-distributed recovery and death rates

The recovery and death rates of infected individuals depend on their age and on time after the infection onset. In this section, we derive an age-dependent immuno-

epidemic model incorporating the effect of total viral load on disease transmission rate. The model is formulated in terms of the number of newly infected individuals and taking into account distributed recovery and death rates and age structure of the population. The demographic factors in an epidemic model is essential in case of vertical transmission of the disease or to study the epidemic progression over a sufficiently long span of time. In this work, our main objective is to study the epidemic progression in a comparatively shorter span of time, and also we do not consider the vertical transmission of the disease. That is why the demographic factor, such as natality and natural (not related to disease) mortality are not considered in this work. Previously, a similar model without age structure was studied in Ghosh et al. (2022).

3.1 Model formulation

Let $J(x,t)$ denote the number of newly infected individuals of age x at time t, while $S(x,t)$, $I(x,t)$, $R(x,t)$, and $D(x,t)$ represent the numbers of susceptible, infected, recovered and dead individuals. Then the total number of infected individuals is given by the following relation:

$$I(x,t) = \int_0^t J(x,\eta)d\eta - R(x,t) - D(x,t). \tag{3.1}$$

We assume that the total population size with a specific age x remains unaltered, that is,

$$S(x,t) + I(x,t) + R(x,t) + D(x,t) = S_0(x),$$

where $S_0(x)$ is the initial age-dependent distribution of the population, which is considered as a given function of x. Differentiating (3.1) with respect to t and taking into account the last equality, we get:

$$\frac{\partial S(x,t)}{\partial t} = -J(x,t).$$

Suppose that the infectivity of an infected individual of age x is determined by the age-dependent viral load $W(x)$. Then the total infectivity of the population is described by the integral $\int_0^\infty W(y)I(y,t)dy$. The susceptibility to infection depends on the age group with the coefficient $\alpha(x)$. Therefore, the disease transmission rate is determined by their product. Hence, we can write

$$\frac{\partial S(x,t)}{\partial t} = -\alpha(x)S(x,t)\int_0^\infty W(y)I(y,t)dy \ \ (\equiv -J(x,t)).$$

The right-hand side of this equation represents the rate of infection progression in the population which takes into account that susceptible $S(x,t)$ of age group x can be infected by all other age groups.

Let $r(x, t-\eta)$ and $d(x, t-\eta)$ be the recovery and death rates for individuals of age x, depending on the time-since-infection $t-\eta$. Then the number of infected individuals of age x, who will recover at time t is given by the integral:

$$\int_0^t r(x, t-\eta) J(x, \eta) d\eta.$$

Similarly, we determine the number of infected individuals of age x, who will die at time t:

$$\int_0^t d(x, t-\eta) J(x, \eta) d\eta.$$

Hence, from (3.1) we obtain the rate of change of the number of infected individuals:

$$\frac{\partial I(x,t)}{\partial t} = \alpha(x) S(x,t) \int_0^\infty W(y) I(y,t) dy - \int_0^t r(x, t-\eta) J(x, \eta) d\eta - \int_0^t d(x, t-\eta) J(x, \eta) d\eta.$$

The rates of change of $R(x,t)$ and $D(x,t)$ are given by the equations:

$$\frac{\partial R(x,t)}{\partial t} = \int_0^t r(x, t-\eta) J(x, \eta) d\eta, \quad \frac{\partial D(x,t)}{\partial t} = \int_0^t d(x, t-\eta) J(x, \eta) d\eta.$$

Thus, we obtain the following system of equations:

$$\frac{\partial S(x,t)}{\partial t} = -\alpha(x) S(x,t) \int_0^\infty W(y) I(y,t) dy \quad (\equiv -J(x,t)), \tag{3.2a}$$

$$\frac{\partial I(x,t)}{\partial t} = \alpha(x) S(x,t) \int_0^\infty W(y) I(y,t) dy - \int_0^t r(x, t-\eta) J(x, \eta) d\eta - \int_0^t d(x, t-\eta) J(x, \eta) d\eta, \tag{3.2b}$$

$$\frac{\partial R(x,t)}{\partial t} = \int_0^t r(x, t-\eta) J(x, \eta) d\eta, \tag{3.2c}$$

$$\frac{\partial D(x,t)}{\partial t} = \int_0^t d(x, t-\eta) J(x, \eta) d\eta, \tag{3.2d}$$

with the initial condition:

$$S(x,0) = S_0(x) > 0, \quad I(x,0) = I_0(x) > 0, \quad R(x,0) = 0 \text{ and } D(x,0) = 0. \tag{3.3}$$

We note that, $S(x,t) + I(x,t) + R(x,t) + D(x,t) = S_0(x) + I_0(x)$ for all x, t under consideration. It is important to mention here that the immunological model is used

to determine how the total viral load $W(x)$ depends on age-dependent immunological parameters.

In what follows we assume that the recovery and death rates satisfy the following inequality

$$\int_{\eta}^{t_0} (r(x, t-\eta) + d(x, t-\eta))dt \leq 1 \tag{3.4}$$

for any η and t_0, $t_0 > \eta$ and x. This condition means that the total number of recovered and dead individuals among those infected at time η remains less than $J(x, \eta)$.

3.2 Existence and uniqueness of solution

In this section we will prove the existence and uniqueness of solution of system (3.2) for $(x, t) \in [0, Q] \times [0, \mathcal{T}_f]$, where $Q, \mathcal{T}_f \in (0, \infty)$, Q is an upper bound of human age. Then system (3.2) reduces to the following one:

$$\frac{\partial S(x,t)}{\partial t} = -\alpha(x)S(x,t)\int_0^Q W(y)I(y,t)dy \quad (\equiv -J(x,t)), \tag{3.5a}$$

$$\frac{\partial I(x,t)}{\partial t} = \alpha(x)S(x,t)\int_0^Q W(y)I(y,t)dy - \int_0^t r(x,t-\eta)J(x,\eta)d\eta - \int_0^t d(x,t-\eta)J(x,\eta)d\eta, \tag{3.5b}$$

$$\frac{\partial R(x,t)}{\partial t} = \int_0^t r(x,t-\eta)J(x,\eta)d\eta, \tag{3.5c}$$

$$\frac{\partial D(x,t)}{\partial t} = \int_0^t d(x,t-\eta)J(x,\eta)d\eta, \tag{3.5d}$$

with the initial conditions given in (3.3). We assume that the coefficients and initial conditions are continuous and positive. Note that if $J(x,t)$ is uniquely determined then the equations (3.5c) and (3.5d) have unique solutions. Hence, it is sufficient to prove the existence and uniqueness of solution for the two equations (3.5a)-(3.5b).

Before proving the existence and uniqueness of solution, we will verify that the solutions of system (3.5) with initial conditions (3.3) are positive and bounded.

Lemma 1 *If condition (3.4) is satisfied, then any solution $S(x,t)$, $I(x,t)$, $R(x,t)$, and $D(x,t)$ of system (3.5) with initial condition (3.3) satisfies the inequality*

$$0 \leq \mathcal{A} \leq S_0(x) + I_0(x),$$

where $\mathcal{A} = \{S(x,t), I(x,t), R(x,t), D(x,t)\}$.

Proof From (3.5a) we observe that if $S(x,t_*) = 0$ for some x and t_*, then $\frac{\partial S(x,t)}{\partial t}\Big|_{t=t_*} = 0$. This shows that $S(x,t) \geq 0$ for all $x, t > 0$. From (3.5c), (3.5d) we conclude that $R(x,t)$ and $D(x,t)$ also remain positive for all x, t.

It follows from equation (3.1) that

$$I(x,t_0)=\int_0^{t_0}J(x,\eta)d\eta-R(x,t_0)-D(x,t_0), \tag{3.6}$$

for some $t=t_0>0$. Integrating (3.5c), (3.5d) with respect to t from 0 to t_0 and taking into account the initial conditions $R(x,0)=D(x,0)=0$, we get

$$R(x,t_0)+D(x,t_0)=\int_0^{t_0}\left(\int_0^{t}\big(r(x,t-\eta)+d(x,t-\eta)\big)J(x,\eta)d\eta\right)dt.$$

Changing the order of integration and taking into account inequality (3.4), we find

$$\begin{aligned}R(x,t_0)+D(x,t_0)&=\int_0^{t_0}\left(\int_\eta^{t_0}\big(r(x,t-\eta)+d(x,t-\eta)\big)dt\right)J(x,\eta)d\eta\\&\le\int_0^{t_0}J(x,\eta)d\eta.\end{aligned}$$

Together with (3.6), this gives $I(x,t_0)\ge 0$. Furthermore,

$$S(x,t)+I(x,t)+R(x,t)+D(x,t)=S_0(x)+I_0(x).$$

Thus, any solution of system (3.5a)-(3.5d) lies between 0 and $S_0(x)+I_0(x)$. □

We now proceed to the proof of the existence theorem.

Theorem 1 *There exists a unique solution (S,I) of system (3.5a)-(3.5b) in the domain Ω^2, where $\Omega\subset C\big([0,Q]\times[0,\mathcal{T}_f],\ \mathbb{R}\big)$ is defined by*

$$\Omega:=\Big\{T\in C\big([0,Q]\times[0,\mathcal{T}_f],\mathbb{R}\big):0\le T(x,t)\le S_0(x)+I_0(x),\forall(x,t)\in[0,Q]\times[0,\mathcal{T}_f]\Big\}.$$

To prove this theorem we need a mathematical setup of complete metric space, which is defined properly in the following lemma.

Lemma 2 *$\big(\Omega,d\big)$ is a complete metric space with respect to the metric $d(T_1,T_2)$ defined by*

$$d(T_1,T_2)=\sup_{(x,t)\in[0,Q]\times[0,\mathcal{T}_f]}\Big\{e^{-\gamma t}|T_1(x,t)-T_2(x,t)|\Big\},$$

where $\gamma>0$ is a constant.

Proof Note that Ω is a closed subset of $C\big([0,Q]\times[0,\mathcal{T}_f],\ \mathbb{R}\big)$. Since $C\big([0,Q]\times[0,\mathcal{T}_f],\ \mathbb{R}\big)$ is a complete metric space with respect to the supremum metric

$$d_{\sup}(T_1,T_2)=\sup_{(x,t)\in[0,Q]\times[0,\mathcal{T}_f]}\{|T_1(x,t)-T_2(x,t)|\},$$

then $(\Omega, d_{\sup})$ is a complete metric space.

Next, we have the following relation between the two metrics d and $d_{\sup}$ on Ω

$$e^{-\gamma \mathcal{T}_f} d_{\sup}(T_1, T_2) \leq d(T_1, T_2) \leq d_{\sup}(T_1, T_2),$$

which implies that $d_{\sup}$ and d are equivalent metrics. This proves that (Ω, d) is a complete metric space. □

We now proceed to prove the existence and uniqueness of solution of system (3.5a)-(3.5b) in the metric space (Ω, d). For any given function $T(x,t) \in \Omega$ and for every x, equation

$$\frac{\partial S(x,t)}{\partial t} = -\alpha(x) S(x,t) \int_0^Q W(y) T(y,t) dy \tag{3.7}$$

with initial condition $S(x,0) = S_0(x)$ has a unique solution

$$S_T(x,t) = S_0(x) e^{-\alpha(x) \int_0^t \left(\int_0^Q W(y) T(y,\eta) dy \right) d\eta}. \tag{3.8}$$

Note that subscript T is used to denote the unique solution of equation (3.7) for a given function $T(x,t) \in \Omega$. Let us denote

$$J_T(x,t) = \alpha(x) S_T(x,t) \int_0^Q W(y) T(y,t) dy.$$

Then equation

$$\begin{aligned} \frac{\partial I(x,t)}{\partial t} &= \alpha(x) S_T(x,t) \int_0^Q W(y) T(y,t) dy \\ &\quad - \int_0^t \big(r(x, t-\eta) + d(x, t-\eta) \big) J_T(x,\eta) d\eta \end{aligned} \tag{3.9}$$

with $I(x,0) = I_0(x)$ also has a unique solution which can be written in the form

$$I_T(x,t) = I_0(x) + \int_0^t G(x,\eta,T) d\eta, \tag{3.10}$$

where

$$\begin{aligned} G(x,\eta,T) &= \alpha(x) S_0(x) e^{-\alpha(x) \int_0^\eta \left(\int_0^Q W(y) T(y,\xi) dy \right) d\xi} \int_0^Q W(y) T(y,\eta) dy \\ &\quad - \int_0^\eta \Bigg[\big(r(x, \eta-\xi) + d(x, \eta-\xi) \big) \\ &\quad \alpha(x) S_0(x) e^{-\alpha(x) \int_0^\xi \left(\int_0^Q W(y) T(y,\zeta) dy \right) d\zeta} \int_0^Q W(y) T(y,\xi) dy \Bigg] d\xi. \end{aligned} \tag{3.11}$$

Let us now consider the map $\mathcal{L}: (\Omega, d) \to (\Omega, d)$ defined by the equality

$$\mathcal{L}(T)(x,t) = I_0(x) + \int_0^t G(x,\eta,T)d\eta, \tag{3.12}$$

where $G(x,\eta,T)$ is given in (3.11). Before proceeding further, we verify that $\mathcal{L}$ maps (Ω, d) into itself.

Lemma 3 *The map $\mathcal{L}: (\Omega, d) \to (\Omega, d)$ is well-defined.*

Proof From (3.8) we obtain

$$\frac{\partial S_T(x,t)}{\partial t} = -\alpha(x)S_0(x)e^{-\alpha(x)\int_0^t \left(\int_0^Q W(y)T(y,\eta)dy\right)d\eta}\int_0^Q W(y)T(y,t)dy.$$

Substituting this relation into (3.11), we can write

$$G(x,\eta,T) = -\left[\frac{\partial S_T(x,\eta)}{\partial \eta} - \int_0^\eta \left(r(x,\eta-\xi)+d(x,\eta-\xi)\right)\frac{\partial S_T(x,\xi)}{\partial \xi}d\xi\right].$$

Next,

$$\int_0^t G(x,\eta,T)d\eta = -\left[\int_0^t \frac{\partial S_T(x,\eta)}{\partial \eta}d\eta - \int_0^t\int_0^\eta \left(r(x,\eta-\xi)+d(x,\eta-\xi)\right)\frac{\partial S_T(x,\xi)}{\partial \xi}d\xi d\eta\right].$$

Changing the order of integration in the right-hand side, we get

$$\begin{aligned}\int_0^t G(x,\eta,T)d\eta &= -\left[\int_0^t \frac{\partial S_T(x,\eta)}{\partial \eta}d\eta - \int_0^t\left(\int_\xi^t \left(r(x,\eta-\xi)\right.\right.\right.\\ &\quad \left.\left.\left.+d(x,\eta-\xi)\right)d\eta\right)\frac{\partial S_T(x,\xi)}{\partial \xi}d\xi\right]\\ &= -\left[\int_0^t\left(1-\int_\xi^t \left(r(x,\eta-\xi)+d(x,\eta-\xi)\right)d\eta\right)\frac{\partial S_T(x,\xi)}{\partial \xi}d\xi\right].\end{aligned}$$

Note that $\frac{\partial S_T(x,\xi)}{\partial \xi} \le 0$ and following condition (3.4), we conclude that

$$\int_0^t G(x,\eta,T)d\eta \le -\int_0^t \frac{\partial S_T(x,\xi)}{\partial \xi}d\xi = S_0(x) - S_T(x,t) \le S_0(x).$$

This implies

$$\mathcal{L}(T)(x,t) = I_0(x) + \int_0^t G(x,\eta,T)d\eta \le I_0(x) + S_0(x).$$

Let us also note that if $T_1(x,t), T_2(x,t) \in \Omega$ and $T_1(x,t) = T_2(x,t)$, then $S_{T_1}(x,t) = S_{T_2}(x,t)$ and consequently $G(x,\eta,T_1) = G(x,\eta,T_2)$. Hence the map $\mathcal{L}$ is well-defined. □

Next, we prove that the map $\mathcal{L}: (\Omega, d) \to (\Omega, d)$ defined in (3.12) is a contraction.

Lemma 4 *The map $\mathcal{L}: (\Omega, d) \to (\Omega, d)$ defined in (3.12) is a contraction map.*

Proof For any two functions $T_1(x,t),\ T_2(x,t) \in \Omega$,

$$\big|\mathcal{L}(T_1)(x,t) - \mathcal{L}(T_2)(x,t)\big| \le \int_0^t \big|G(x,\eta,T_1) - G(x,\eta,T_2)\big| d\eta.$$

Then we have the following estimate:

$$\begin{aligned}\big|G(x,\eta,T_1) - G(x,\eta,T_2)\big| = \alpha(x)S_0(x)\Bigg|&\Bigg[e^{-\alpha(x)\int_0^\eta \tilde{T}_1(\xi)d\xi}\tilde{T}_1(\eta)\\ &- \int_0^\eta (r(x,\eta-\xi)+d(x,\eta-\xi))e^{-\alpha(x)\int_0^\xi \tilde{T}_1(\zeta)d\zeta}\tilde{T}_1(\xi)d\xi\Bigg]\\ &-\Bigg[e^{-\alpha(x)\int_0^\eta \tilde{T}_2(\xi)d\xi}\tilde{T}_2(\eta)\\ &- \int_0^\eta (r(x,\eta-\xi)+d(x,\eta-\xi))e^{-\alpha(x)\int_0^\xi \tilde{T}_2(\zeta)d\zeta}\tilde{T}_2(\xi)d\xi\Bigg]\Bigg|,\end{aligned}$$

where

$$\tilde{T}_j(\xi) = \int_0^Q W(y)T_j(y,\xi)dy, \quad j = 1,2.$$

Therefore,

$$\begin{aligned}\big|G(x,\eta,T_1) - G(x,\eta,T_2)\big| = \alpha(x)S_0(x)\Big|&e^{-\alpha(x)\int_0^\eta \tilde{T}_1(\xi)d\xi}\big(\tilde{T}_1(\eta) - \tilde{T}_2(\eta)\big)\\ &+\int_0^\eta (r(x,\eta-\xi)+d(x,\eta-\xi))e^{-\alpha(x)\int_0^\xi \tilde{T}_1(\zeta)d\zeta}\Big(\tilde{T}_2(\xi) - \tilde{T}_1(\xi)\Big)d\xi\\ &+\big(e^{-\alpha(x)\int_0^\eta \tilde{T}_1(\xi)d\xi} - e^{-\alpha(x)\int_0^\eta \tilde{T}_2(\xi)d\xi}\big)\tilde{T}_2(\eta) + \int_0^\eta (r(x,\eta-\xi)\\ &+d(x,\eta-\xi))\big(e^{-\alpha(x)\int_0^\xi \tilde{T}_2(\zeta)d\zeta} - e^{-\alpha(x)\int_0^\xi \tilde{T}_1(\zeta)d\zeta}\big)\tilde{T}_2(\xi)d\xi\Big|,\end{aligned}$$

Using the inequalities

$$\big|e^{-x} - e^{-y}\big| \le \big|x-y\big|, \quad \big|e^{-x}\big| \le 1$$

for any $x, y \geq 0$, we get

$$\begin{aligned}\left|G(x,\eta,T_1)-G(x,\eta,T_2)\right| \leq \alpha(x)S_0(x)\Big(&\left|\tilde{T}_1(\eta)-\tilde{T}_2(\eta)\right| \\ &+\int_0^\eta (r(x,\eta-\xi)+d(x,\eta-\xi))\left|\tilde{T}_2(\xi)-\tilde{T}_1(\xi)\right|d\xi \\ &+\alpha(x)\tilde{T}_2(\eta)\int_0^\eta \left|\tilde{T}_1(\xi)-\tilde{T}_2(\xi)\right|d\xi+\int_0^\eta \Big(r(x,\eta-\xi) \\ &+d(x,\eta-\xi)\Big)\Big(\alpha(x)\int_0^\xi \left|\tilde{T}_2(\zeta)-\tilde{T}_1(\zeta)\right|d\zeta\Big)\tilde{T}_2(\xi)d\xi\Big).\end{aligned}$$

Since, $T_j(x,t) \leq S_0(x)+I_0(x), \forall (x,t) \in [0, Q] \times [0, \mathcal{T}_f]$, we get

$$\tilde{T}_j(\xi) \leq M, \quad j = 1, 2,$$

where

$$M = (S_0(x)+I_0(x))\int_0^Q W(y)dy.$$

Next,

$$\left|\tilde{T}_1(\eta)-\tilde{T}_2(\eta)\right| \leq \int_0^Q W(y)\left|T_1(y,\eta)-T_2(y,\eta)\right|dy \leq e^{\gamma\eta}d(T_1,T_2)\int_0^Q W(y)dy.$$

Using this inequality and condition (3.4), we can write

$$\begin{aligned}\left|G(x,\eta,T_1)-G(x,\eta,T_2)\right| &\leq \alpha(x)S_0(x)d(T_1,T_2)\int_0^Q W(y)dy\Big[e^{\gamma\eta}+\int_0^\eta e^{\gamma\xi}d\xi \\ &\quad+\alpha(x)M\int_0^\eta e^{\gamma\xi}d\xi+\alpha(x)M\int_0^\eta\int_0^\xi e^{\gamma\zeta}d\zeta d\xi\Big] \\ &\leq \alpha(x)S_0(x)d(T_1,T_2)\int_0^Q W(y)dy\Big[e^{\gamma\eta}+\frac{1}{\gamma}\Big(e^{\gamma\eta}-1\Big) \\ &\quad+\alpha(x)M\frac{1}{\gamma}\Big(e^{\gamma\eta}-1\Big)+\alpha(x)M\frac{1}{\gamma^2}\Big(e^{\gamma\eta}-1\Big)\Big] \\ &\leq \alpha(x)S_0(x)d(T_1,T_2)\Big[e^{\gamma\eta}\Big(1+\frac{1}{\gamma}+\frac{\alpha(x)M}{\gamma} \\ &\quad+\frac{\alpha(x)M}{\gamma^2}\Big)\Big]\int_0^Q W(y)dy.\end{aligned}$$

This implies the estimate

$$\begin{aligned}\left|\mathcal{L}(T_1)(x,t)-\mathcal{L}(T_2)(x,t)\right| &\leq \alpha(x)S_0(x)d(T_1,T_2)\bigg(1+\frac{1+\alpha(x)M}{\gamma}\\ &\quad+\frac{\alpha(x)M}{\gamma^2}\bigg)\int_0^t e^{\gamma\eta}d\eta\int_0^Q W(y)dy\\ &= \alpha(x)S_0(x)d(T_1,T_2)\bigg(1+\frac{1+\alpha(x)M}{\gamma}\\ &\quad+\frac{\alpha(x)M}{\gamma^2}\bigg)\frac{e^{\gamma t}-1}{\gamma}\int_0^Q W(y)dy.\end{aligned}$$

Hence,

$$\begin{aligned}e^{-\gamma t}\left|\mathcal{L}(T_1)(x,t)-\mathcal{L}(T_2)(x,t)\right| &\leq \bigg[\alpha(x)S_0(x)\bigg(\frac{1}{\gamma}+\frac{1+\alpha(x)M}{\gamma^2}\\ &\quad+\frac{\alpha(x)M}{\gamma^3}\bigg)\int_0^Q W(y)dy\bigg]d(T_1,T_2).\end{aligned}$$

Since $\alpha(x)$, $S_0(x)$ are positive continuous functions on $[0,\, Q]$, there exists positive constants M_α and M_s such that

$$\alpha(x)\leq M_\alpha \quad , \quad S_0(x)\leq M_s,$$

for all $x\in[0,\, Q]$. Let

$$\int_0^Q W(y)dy = M_w.$$

Then we have

$$e^{-\gamma t}\left|\mathcal{L}(T_1)(x,t)-\mathcal{L}(T_2)(x,t)\right| \leq \bigg[M_\alpha M_s M_w\bigg(\frac{1}{\gamma}+\frac{1+M_\alpha M}{\gamma^2}+\frac{M_\alpha M}{\gamma^3}\bigg)\bigg]d(T_1,T_2).$$

Taking the supremum from both sides, we get

$$d(\mathcal{L}(T_1),\mathcal{L}(T_2))\leq\bigg[M_\alpha M_s M_w\bigg(\frac{1}{\gamma}+\frac{1+M_\alpha M}{\gamma^2}+\frac{M_\alpha M}{\gamma^3}\bigg)\bigg]d(T_1,T_2).$$

We now choose the value of $\gamma>0$ large enough so that

$$M_\alpha M_s M_w\bigg(\frac{1}{\gamma}+\frac{1+M_\alpha M}{\gamma^2}+\frac{M_\alpha M}{\gamma^3}\bigg)<1.$$

Consequently,

$$\mathcal{L}: (\Omega, d) \to (\Omega, d)$$

is a contraction map on the complete metric space (Ω, d). □

To finish the proof of existence of solution, we use the following theorem.

Theorem 2 *Let (X, d) be a complete metric space and let $T : X \to X$ be a contraction mapping on X. Then T has a unique fixed point $x \in X$ (such that $T(x) = x$).*

It follows from this theorem that the map $\mathcal{L}$ has a unique fixed point. Thus, there exists a unique function $T_u \in \Omega \subset C\big([0, Q] \times [0, \mathcal{T}_f], \mathbb{R}\big)$ satisfying the equality

$$T_u(x, t) = I_0(x) + \int_0^t G(x, \eta, T_u) d\eta,$$

where $G(x, \eta, T_u)$ is given in (3.11). Besides, we note that $G(x, \eta, T)$ is a continuous function. Hence, the derivative $\frac{\partial T_u(x,t)}{\partial t}$ exists. This completes the proof of the existence and uniqueness of solution of system (3.5a)-(3.5d).

4 Age-dependent immuno-epidemic model with time-independent recovery and death rates

In this section we reduce the immuno-epidemic model (3.2a)–(3.2d) to a SIR type model assuming that recovery and death rates are age-dependent but they do not depend on time.

4.1 Reduction to SIR model

In a particular case, consider the recovery and death rates $r(x, t-\eta)$ and $d(x, t-\eta)$ in the form

$$r(x, t-\eta) = \begin{cases} \gamma(x), & t - \tau(x) < \eta \le t \\ 0, & \eta < t - \tau(x) \end{cases}, \quad d(x, t-\eta) = \begin{cases} \delta(x), & t - \tau(x) < \eta \le t \\ 0, & \eta < t - \tau(x) \end{cases}, \tag{4.1}$$

where $\tau(x) > 0$ is the disease duration of an infected individual of age x, $\gamma(x)$ and $\delta(x)$ are some functions of x. Substituting these functions into (3.2c) and (3.2d), we get

$$\frac{\partial R(x,t)}{\partial t} = \gamma(x) \int_{t-\tau(x)}^{t} J(x, \eta) d\eta, \quad \frac{\partial D(x,t)}{\partial t} = \delta(x) \int_{t-\tau(x)}^{t} J(x, \eta) d\eta. \tag{4.2}$$

Integrating these two equations from $t-\tau(x)$ to t, we obtain the following relations:

$$R(x,t)-R(x,t-\tau(x))=\gamma(x)\int_{t-\tau(x)}^{t}\left(\int_{s-\tau(x)}^{s}J(x,\eta)d\eta\right)ds,$$

and

$$D(x,t)-D(x,t-\tau(x))=\delta(x)\int_{t-\tau(x)}^{t}\left(\int_{s-\tau(x)}^{s}J(x,\eta)d\eta\right)ds.$$

Since $\tau(x)>0$ is the disease duration of an infected individual of age x, then the expressions $(R(x,t)-R(x,t-\tau(x)))$ and $(D(x,t)-D(x,t-\tau(x)))$ represent the number of recovered and dead individuals of age x during the time interval $(t-\tau(x),\ t)$, respectively. Hence, (3.1) can be written as follows:

$$\begin{aligned}I(x,t)=&\int_{t-\tau(x)}^{t}J(x,\eta)d\eta-(R(x,t)-R(x,t-\tau(x)))\\&-(D(x,t)-D(x,t-\tau(x))).\end{aligned}\tag{4.3}$$

Therefore, from (4.3), we conclude that

$$I(x,t)=\int_{t-\tau(x)}^{t}J(x,\eta)d\eta-(\gamma(x)+\delta(x))\int_{t-\tau(x)}^{t}\left(\int_{s-\tau(x)}^{s}J(x,\eta)d\eta\right)ds.\tag{4.4}$$

Next, from (3.2b) and (4.4),

$$\begin{aligned}\frac{\partial I(x,t)}{\partial t}&=\alpha(x)S(x,t)\int_0^\infty W(y)I(y,t)dy-(\gamma(x)+\delta(x))\int_{t-\tau(x)}^{t}J(x,\eta)d\eta\\&=\alpha(x)S(x,t)\int_0^\infty W(y)I(y,t)dy\\&\quad-(\gamma(x)+\delta(x))\left[I(x,t)+(\gamma(x)+\delta(x))\int_{t-\tau(x)}^{t}\left(\int_{s-\tau(x)}^{s}J(x,\eta)d\eta\right)ds\right].\end{aligned}$$

If we suppose that, for every x, $(\gamma(x)+\delta(x))$ is small enough and we neglect the term involving $(\gamma(x)+\delta(x))^2$, then we obtain

$$\frac{\partial I(x,t)}{\partial t}\approx\alpha(x)S(x,t)\int_0^\infty W(y)I(y,t)dy-(\gamma(x)+\delta(x))I(x,t).$$

In this case, system (3.2a)-(3.2d) is reduced to the age-dependent SIR-type model:

$$\frac{\partial S(x,t)}{\partial t} = -\alpha(x)S(x,t)\int_0^\infty W(y)I(y,t)dy, \tag{4.5a}$$

$$\frac{\partial I(x,t)}{\partial t} = \alpha(x)S(x,t)\int_0^\infty W(y)I(y,t)dy - (\gamma(x)+\delta(x))I(x,t), \tag{4.5b}$$

$$\frac{\partial R(x,t)}{\partial t} = \gamma(x)I(x,t), \quad \frac{\partial D(x,t)}{\partial t} = \delta(x)I(x,t). \tag{4.5c}$$

4.2 Basic reproduction number

Let us study stability of the disease-free equilibrium $\mathcal{E}_0 = (S_0(x), 0, 0, 0)$. Consider the perturbation of this solution:

$$S(x,t) = S_0(x) + \tilde{S}(x,t);\ I(x,t) = \tilde{I}(x,t);\ R(x,t) = \tilde{R}(x,t);\ D(x,t) = \tilde{D}(x,t).$$

Then the linearized system corresponding to (4.5a)-(4.5c) with respect to the above perturbation takes the form:

$$\frac{\partial \tilde{S}(x,t)}{\partial t} = -\alpha(x)S_0(x)\int_0^\infty W(y)\tilde{I}(y,t)dy, \tag{4.6}$$

$$\frac{\partial \tilde{I}(x,t)}{\partial t} = \alpha(x)S_0(x)\int_0^\infty W(y)\tilde{I}(y,t)dy - \gamma(x)\tilde{I}(x,t) - \delta(x)\tilde{I}(x,t), \tag{4.7}$$

$$\frac{\partial \tilde{R}(x,t)}{\partial t} = \gamma(x)\tilde{I}(x,t), \quad \frac{\partial \tilde{D}(x,t)}{\partial t} = \delta(x)\tilde{I}(x,t). \tag{4.8}$$

We search for a solution of system (4.6)-(4.8) of the form

$$\tilde{S}(x,t) = e^{\lambda t}\phi_1(x);\ \tilde{I}(x,t) = e^{\lambda t}\phi_2(x);\ \tilde{R}(x,t) = e^{\lambda t}\phi_3(x);\ \tilde{D}(x,t) = e^{\lambda t}\phi_4(x).$$

Substituting this solution into (4.7), we obtain

$$\lambda\phi_2(x) = \alpha(x)S_0(x)\int_0^\infty W(y)\phi_2(y)dy - \gamma(x)\phi_2(x) - \delta(x)\phi_2(x). \tag{4.9}$$

Let

$$\Lambda = \int_0^\infty W(y)\phi_2(y)dy. \tag{4.10}$$

Then we have

$$\phi_2(x) = \frac{\Lambda\alpha(x)S_0(x)}{(\lambda+\gamma(x)+\delta(x))}.$$

Inserting it into (4.10), we get

$$\Lambda = \Lambda \int_0^\infty \frac{W(y)\alpha(y)S_0(y)}{(\lambda + \gamma(y) + \delta(y))} dy.$$

Since we are looking for nonzero solution, $\Lambda \neq 0$, we obtain the following characteristic equation

$$1 = \int_0^\infty \frac{W(y)\alpha(y)S_0(y)}{(\lambda + \gamma(y) + \delta(y))} dy.$$

Set

$$\mathcal{G}(\lambda) = \int_0^\infty \frac{W(y)\alpha(y)S_0(y)}{(\lambda + \gamma(y) + \delta(y))} dy.$$

We define the basic reproduction number $\mathcal{R}_0$ as $\mathcal{G}(0)$:

$$\mathcal{R}_0 = \int_0^\infty \frac{W(y)\alpha(y)S_0(y)}{(\gamma(y) + \delta(y))} dy.$$

Theorem 3 *If $\mathcal{R}_0 > 1$, then the disease-free equilibrium $\mathcal{E}_0$ is unstable. If $\mathcal{R}_0 < 1$, then $\mathcal{E}_0$ is locally asymptotically stable.*

Proof Let $\mathcal{R}_0 > 1$. Observe that $\mathcal{G}(\lambda)$ is a decreasing function of λ, if λ is considered as a real variable. Now, $\mathcal{R}_0 > 1$ implies $\mathcal{G}(0) > 1$, also $\lim_{\lambda\to\infty} \mathcal{G}(\lambda) = 0$. Thus, we can conclude that there is a real positive number λ^* such that $\mathcal{G}(\lambda^*) = 1$. Hence, the disease-free equilibrium is unstable.

Let $\mathcal{R}_0 < 1$. For any $\lambda = a + ib$ with $a \geq 0$ we have

$$|\mathcal{G}(\lambda)| \leq \mathcal{G}(a) \leq \mathcal{G}(0) = \mathcal{R}_0 < 1.$$

This result implies that the system has no eigenvalue with nonnegative real part. Hence, the disease-free equilibrium is locally asymptotically stable. □

Remark If $S_0(x) = N$, $\gamma(x) = \gamma_0$, $\delta(x) = \delta_0$, $\alpha(x) = \beta$, and if we replace $W(y)$ by the Dirac delta-function $\delta(y - x)$, then $\mathcal{R}_0 = \frac{\beta N}{\gamma_0 + \delta_0}$. We obtain the basic reproduction number for the conventional SIR model with a homogeneous population.

4.3 Final size of the epidemic

Let $\lim_{t\to\infty} S(x, t) = S_f(x)$. We divide (4.5a) by $S(x, t)$ and integrate with respect to t from 0 to ∞:

$$\ln \frac{S_f(x)}{S_0(x)} = -\alpha(x) \int_0^\infty \int_0^\infty W(y)I(y, t)dydt = -\alpha(x) \int_0^\infty W(y)\left(\int_0^\infty I(y, t)dt \right)dy. \tag{4.11}$$

Adding (4.5a), (4.5b) and then integrating with respect to t from 0 to ∞, we get

$$S_f(x) - S_0(x) = -(\gamma(x) + \delta(x)) \int_0^\infty I(x,t)dt. \tag{4.12}$$

Substituting (4.12) into (4.11), we obtain the following equality:

$$\ln \frac{S_f(x)}{S_0(x)} = -\alpha(x) \int_0^\infty W(y) \frac{S_0(y) - S_f(y)}{\gamma(y) + \delta(y)} dy.$$

Let

$$A = \int_0^\infty W(y) \frac{S_0(y) - S_f(y)}{\gamma(y) + \delta(y)} dy.$$

Then

$$S_f(x) = S_0(x) e^{-A\alpha(x)}.$$

We substitute $S_f(x)$ in the expression for A:

$$A = \int_0^\infty W(y) \frac{S_0(y)(1 - e^{-A\alpha(y)})}{\gamma(y) + \delta(y)} dy.$$

Let

$$\mathcal{F}(A) = A - \int_0^\infty W(y) \frac{S_0(y)(1 - e^{-A\alpha(y)})}{\gamma(y) + \delta(y)} dy.$$

Clearly, $\mathcal{F}(0) = 0$ and

$$\mathcal{F}'(A) = 1 - \int_0^\infty W(y) \frac{S_0(y)\alpha(y) e^{-A\alpha(y)}}{\gamma(y) + \delta(y)} dy.$$

Hence,

$$\mathcal{F}'(0) = 1 - \int_0^\infty W(y) \frac{S_0(y)\alpha(y)}{\gamma(y) + \delta(y)} dy = 1 - \mathcal{R}_0.$$

Suppose that $\mathcal{R}_0 > 1$. Then, $\mathcal{F}'(0) = 1 - \mathcal{R}_0 < 0$, and $\lim_{A\to\infty} \mathcal{F}(A) = \infty$. Moreover, $\mathcal{F}'(A)$ is a strictly increasing function of A. Hence, the equation $\mathcal{F}(A) = 0$ has unique positive root. Thus, if $\mathcal{R}_0 > 1$, then the final size of epidemic is given by the relation:

$$S_f(x) = S_0(x) e^{-A_* \alpha(x)}, \tag{4.13}$$

where A_* is the unique positive solution of equation $\mathcal{F}(A) = 0$.

5 Age-dependent immuno-epidemic model with delayed recovery and death rates

As before, we consider in this section a fixed disease duration but different recovery and death distribution which allow us to obtain an age-dependent delay model.

5.1 Reduction to the delay model

We assume that the disease duration for an infected individual with age x is $\tau(x)$. Set

$$r(x,t-\eta) = r_0(x)\,\delta(t-\eta-\tau(x)), \quad d(x,t-\eta) = d_0(x)\,\delta(t-\eta-\tau(x)),$$

where $r_0(x) + d_0(x) = 1$ for all x, and δ is the Dirac delta-function. Then

$$\frac{\partial R(x,t)}{\partial t} = \int_0^t r(x,t-\eta)J(x,\eta)d\eta = r_0(x)J(x,t-\tau(x))$$

and

$$\frac{\partial D(x,t)}{\partial t} = \int_0^t d(x,t-\eta)J(x,\eta)d\eta = d_0(x)J(x,t-\tau(x)).$$

We assume that $J(x,t) = 0$ for $t < 0$. Integrating the above two equations from 0 to t, we get

$$\begin{aligned} R(x,t) = r_0(x)\int_0^t J(x,s-\tau(x))ds &= r_0(x)\int_{-\tau(x)}^{t-\tau(x)} J(x,y)dy \\ &= r_0(x)\int_0^{t-\tau(x)} J(x,y)dy, \\ D(x,t) = d_0(x)\int_0^t J(x,s-\tau(x))ds &= d_0(x)\int_{-\tau(x)}^{t-\tau(x)} J(x,y)dy \\ &= d_0(x)\int_0^{t-\tau(x)} J(x,y)dy. \end{aligned}$$

Then the model (3.2a)-(3.2d) reduces to the age-dependent delay model:

$$\frac{\partial S(x,t)}{\partial t} = -\alpha(x)S(x,t)\int_0^\infty W(y)I(y,t)dy \quad (= -J(x,t)), \tag{5.1a}$$

$$\frac{\partial I(x,t)}{\partial t} = \alpha(x)S(x,t)\int_0^\infty W(y)I(y,t)dy - J(x,t-\tau(x)), \tag{5.1b}$$

$$\frac{\partial R(x,t)}{\partial t} = r_0(x)J(x,t-\tau(x)), \tag{5.1c}$$

$$\frac{\partial D(x,t)}{\partial t} = d_0(x)J(x,t-\tau(x)). \tag{5.1d}$$

It follows from (3.1) that the number of active cases $I(x,t)$ of age x at time t is given by

$$I(x,t) = \int_{t-\tau(x)}^{t} J(x,\eta)d\eta. \tag{5.2}$$

It can be substituted in the right-hand sides of equations (5.1a) and (5.1b).

5.2 Growth rate and basic reproduction number

In the beginning of epidemic, the change of the number of susceptible can be neglected, $S(x,t) \approx S_0(x)$. From (5.1a), we get

$$J(x,t) = \alpha(x)S_0(x)\int_0^{\infty} W(y)\left(\int_{t-\tau(y)}^{t} J(y,\eta)d\eta\right)dy.$$

Hence, we can write,

$$J(x,t) = \alpha(x)S_0(x)\Omega(t),$$

where

$$\Omega(t) = \int_0^{\infty} W(y)\left(\int_{t-\tau(y)}^{t} J(y,\eta)d\eta\right)dy.$$

Therefore,

$$\Omega(t) = \int_0^{\infty}\int_{t-\tau(y)}^{t} W(y)\alpha(y)S_0(y)\Omega(\eta)d\eta dy.$$

After the change of variables $\xi = t - \eta$ in the integral, we get

$$\Omega(t) = \int_0^{\infty}\int_0^{\tau(y)} W(y)\alpha(y)S_0(y)\Omega(t-\xi)d\xi dy. \tag{5.3}$$

Substituting $\Omega(t) = \Omega_0\, e^{\mu t}$ in the equation (5.3) we get

$$F(\mu) = 1, \tag{5.4}$$

where

$$F(\mu) = \int_0^{\infty}\int_0^{\tau(y)} W(y)\alpha(y)S_0(y)e^{-\mu\xi}d\xi dy.$$

Here, $F(\mu)$ is a decreasing function of μ and converging to 0 as $\mu \to \infty$. Therefore, the equation (5.4) has a positive solution if and only if $F(0) > 1$. Hence, the basic

reproduction number $\mathcal{R}_0$ is given by $F(0)$,

$$\mathcal{R}_0 = \int_0^\infty W(y)\alpha(y)S_0(y)\tau(y)dy.$$

In order to determine an approximate value for the growth rate μ, we take the first two terms of the Taylor expansion of the function $F(\mu)$:

$$F(0) + F'(0)\mu = 1.$$

Hence,

$$\mu = \frac{\mathcal{R}_0 - 1}{\mathcal{R}_1},$$

where

$$\mathcal{R}_1 = \frac{1}{2}\int_0^\infty W(y)\alpha(y)S_0(y)\tau(y)^2dy.$$

In a particular case, if we consider a fixed disease duration, $\tau(x) = \tau$ (constant), then,

$$\mathcal{R}_0 = \tau\sigma, \qquad \mathcal{R}_1 = \frac{\tau^2}{2}\sigma,$$

where

$$\sigma = \int_0^\infty W(y)\alpha(y)S_0(y)dy.$$

Consequently, the growth rate μ is given by the expression

$$\mu = \frac{2(\mathcal{R}_0 - 1)}{\tau\mathcal{R}_0}.$$

Remark For different values of τ, the value of σ can be adjusted to keep the basic reproduction number $\mathcal{R}_0$ fixed, but the growth rate μ will be different. In fact, the growth rate μ decreases for a longer disease duration τ. So, growth rates of the number of infected individuals can be different for the same values of the basic reproduction number.

5.3 Final size of epidemic

As above, set $\lim_{t\to\infty} S(x,t) = S_f(x)$. We divide (5.1a) by $S(x,t)$ and integrate with respect to t from 0 to ∞:

$$\ln\frac{S_f(x)}{S_0(x)} = -\alpha(x)\int_0^\infty\int_0^\infty W(y)I(y,t)dydt = -\alpha(x)\int_0^\infty W(y)\Big(\int_0^\infty I(y,t)dt\Big)dy. \tag{5.5a}$$

Next, integrating (5.2), we get

$$\int_0^\infty I(x,t)dt = \int_0^\infty\Big(\int_{t-\tau(x)}^t J(x,\eta)d\eta\Big)dt = \int_{-\tau(x)}^0\Big(\int_0^{\eta+\tau(x)} J(x,\eta)dt\Big)d\eta + \int_0^\infty\Big(\int_\eta^{\eta+\tau(x)} J(x,\eta)dt\Big)d\eta.$$

Since $J(x,t) = 0$ for all $t \in [-\tau(x),\ 0]$, we can write

$$\int_0^\infty I(x,t)dt = \int_0^\infty\Big(\int_\eta^{\eta+\tau(x)} J(x,\eta)dt\Big)d\eta = \tau(x)\int_0^\infty J(x,\eta)d\eta. \tag{5.6}$$

Integrating the equation (5.1a) with respect to t from 0 to ∞

$$S_0(x) - S_f(x) = \int_0^\infty J(x,t)dt$$

and substituting this relation into (5.6), we obtain the following equality:

$$\int_0^\infty I(x,t)dt = \tau(x)\Big(S_0(x) - S_f(x)\Big). \tag{5.7}$$

Next, from (5.7) and (5.5) it follows that

$$\ln\frac{S_f(x)}{S_0(x)} = -\alpha(x)\int_0^\infty W(y)\tau(y)\Big(S_0(y) - S_f(y)\Big)dy. \tag{5.8}$$

Set

$$B = \int_0^\infty W(y)\tau(y)\Big(S_0(y) - S_f(y)\Big)dy.$$

Then from (5.8) we get

$$S_f(x) = S_0(x)e^{-B\alpha(x)}.$$

We substitute $S_f(x)$ in the expression for B:

$$B = \int_0^\infty W(y)S_0(y)(1 - e^{-B\alpha(y)})\tau(y)dy.$$

Denote

$$\mathcal{G}(B) = B - \int_0^\infty W(y)S_0(y)(1 - e^{-B\alpha(y)})\tau(y)dy.$$

Clearly, $\mathcal{G}(0) = 0$ and

$$\mathcal{G}'(B) = 1 - \int_0^\infty W(y)S_0(y)\alpha(y)e^{-B\alpha(y)}\tau(y)dy.$$

Hence,

$$\mathcal{G}'(0) = 1 - \int_0^\infty W(y)S_0(y)\alpha(y)\tau(y)dy = 1 - \mathcal{R}_0.$$

Suppose that $\mathcal{R}_0 > 1$. Then $\mathcal{G}'(0) = 1 - \mathcal{R}_0 < 0$. Since $\lim_{B\to\infty} \mathcal{G}(B) = \infty$ and $\mathcal{G}'(B)$ is a strictly increasing function of B, then the equation $\mathcal{G}(B) = 0$ has a unique positive root B^*.

Thus, if $\mathcal{R}_0 > 1$, then the final size of epidemic is given by the relation:

$$S_f(x) = S_0(x)e^{-B_*\alpha(x)}, \tag{5.9}$$

where B_* is the unique positive solution of the equation $\mathcal{G}(B) = 0$.

6 Estimation of age-dependent distributed rate functions

In this section we estimate the parameters of the model (3.2) on the basis of epidemiological, clinical and experimental data for COVID-19 during Omicron outbreak. We consider a case study for New Zealand for which the required data are available in the literature (Vattiatio et al. 2022). Age interval is considered 0 and 100 years ($Q = 100$). Estimations are performed using the statistical tools discussed in the Appendix 2 and with the help of MATLAB software.

6.1 Estimation of $S_0(x)$

We estimate the initial age-dependent susceptible population for New Zealand using the census data available in (Wikipedia 2018). In Fig. 1a, the blue bars are the real data of age-specific distribution of the population, $S_0(x)/N$, where N is the total population size $N = 4,699,755$. The red curve is the fitting polynomial $P_S(x)$ obtained using

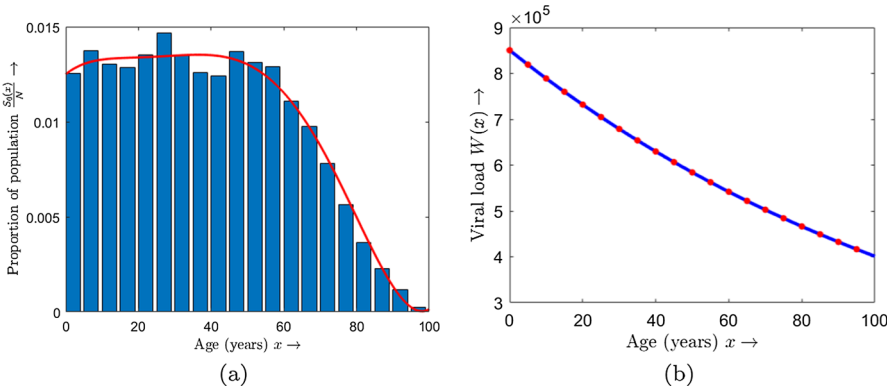

Fig. 1 **a** Population distribution $S_0(x)/N$ with respect to age, N is the total population size, $N = 4,699,755$. **b** Total viral load $W(x)$ for Omicron as a function of individual's age x

the *'Curve Fitting Tool'* in MATLAB:

$$P_S(x) = 2.5666 \times 10^{-11}x^5 - 5.428 \times 10^{-9}x^4 + 3.67 \times 10^{-7}x^3 - 1.086 \times 10^{-5}x^2 + 1539 \times 10^{-4}x + 0.0125,$$

x represents the age of an individual. Hence, the estimated curve for the initial age-dependent susceptible population can be obtained as $NP_S(x)$.

6.2 Estimation of total viral load $W(x)$

We estimate the total viral load for the Omicron strain of SARS-CoV-2 infection depending on the age of infected people. We use the experimental data on viral load for different age groups (Hirotsu et al. 2022). The data points are shown by red dots as shown in Fig. 1b. We fit the data with the exponential function $W(x) = 10^{a-bx}$, where $a = 5.92968$, $b = 0.003263$, and $x \in [0, 100]$. The fitted function $W(x)$ is shown in Fig. 1b by the blue curve.

6.3 Estimation of the susceptibility function $\alpha(x)$

Let $\alpha_p(x)$ be the proportion of people with age x infected by the Omicron variant. It is shown by blue bars in Fig. 2a (Vattiatio et al. 2022). It increases with age, reaches maximum around 25 years and then decreases. The red curve in Fig. 2a represents a gamma distribution fitted to the data using MATLAB function *'fitdist'*:

$$\alpha_p(x) = \frac{1}{q^p \Gamma(p)} x^{p-1} e^{-\frac{x}{q}}.$$

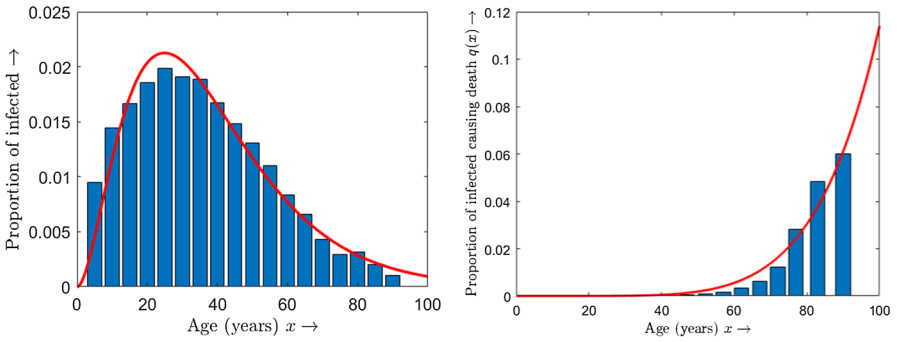

Fig. 2 **a** Age distribution of Omicron infected individuals $\alpha_p(x)$ in New Zealand. **b** Death rate for different age groups

The parameters of the gamma distribution are estimated as $p = 2.91955$ and $q = 12.9779$. We assume that the coefficient $\alpha(x)$ in (3.2a)-(3.2d) is proportional to the function $\alpha_p(x)$, $\alpha(x) = c\alpha_p(x)$, where c is a positive constant determined below.

6.4 Estimation of recovery and death rates

Let $q(x)$ be the probability of an infected individual of age x to die after getting infection (blue bars in Fig. 2b) (Vattiatio et al. 2022). It can be fitted with the function

$$q(x) = 2.126 \times 10^{-12} x^{5.341},$$

(red curve in Fig. 2b).

Denote by $\hat{r}(t)$ and $\hat{d}(t)$ average (age-independent) recovery and death distributions, respectively, as functions of time after the infection onset. Then we approximate the age-dependent recovery and death distributions $r(x,t)$ and $d(x,t)$ as follows:

$$r(x,t) = (1 - q(x))\hat{r}(t); \quad d(x,t) = q(x)\hat{d}(t).$$

We use the functions $\hat{r}(t)$ and $\hat{d}(t)$ determined in Ghosh et al. (2022b) and applicable for different case studies (see Appendix 1):

$$\hat{r}(t) = \frac{0.85}{b_1^{a_1}\Gamma(a_1)} t^{a_1-1} e^{-\frac{t}{b_1}} + \frac{0.15}{d_1^{c_1}\Gamma(c_1)} t^{c_1-1} e^{-\frac{t}{d_1}},$$

$$\hat{d}(t) = \frac{0.94}{b_2^{a_2}\Gamma(a_2)} t^{a_2-1} e^{-\frac{t}{b_2}} + \frac{0.06}{d_2^{c_2}\Gamma(c_2)} t^{c_2-1} e^{-\frac{t}{d_2}},$$

where $a_1 = 32.17136$, $b_1 = 0.2206$, $c_1 = 65.40545$, $d_1 = 0.210$, $a_2 = 36.02855$, $b_2 = 0.57511$, $c_2 = 140.11379$, $d_2 = 0.27636$. The detailed justification behind

considering bi-modal gamma distribution for $\hat{r}(t)$ and $\hat{d}(t)$ can be found in Paul and Lorin (2021).

7 Numerical simulation

In this section we perform some numerical simulations to validate the proposed model and to compare the complete model with the two reduced models.

7.1 Influence of $S_0(x)$

In order to study the influence of the initial age-dependent population distribution on epidemic progression, we consider three hypothetical functions representing the age-dependent initial susceptible population distribution $S_0(x)$, as shown in Fig. 3a by different colors. These cases differ by the proportion of younger age groups with the same total population (integral).

Since the initial age distribution of infected individuals is unknown, and it is probably does not essentially influence infection progression, we set $I_0(x) = 1$ for $x =$ even and $I_0(x) = 0$, otherwise. We have taken $\alpha(x) = c\alpha_p(x)$, where $c = 4.5 \times 10^{-12}$, $N = 10^7$, where $\alpha_p(x)$ and other distributions are estimated in the previous section.

We carry out numerical simulation of system (3.2a)-(3.2d) and characterize infection progression by the total number of newly infected individuals for all age groups:

$$\bar{J}(t) = \int_0^{100} J(x,t)dx.$$

In Fig. 3b we observe that the maximum number of infected and the time to maximum can change significantly depending on the initial age-dependent distribution of the susceptible population.

The blue curve in Fig. 3a corresponds to the population distribution in Fig. 1a. If the proportion of the young age groups increases (green curves), then the maximal number of newly infected individuals also increases while the time to maximum decreases. This is related to higher infection transmission by younger population (Fig. 1b). In the case of a smaller proportion of these age groups (red curves), the maximal number of new infections decreases and the time to maximum increases.

7.2 Comparison among the models (3.2), (4.5), and (5.1)

In this subsection, we compare the epidemic progression determined by the three different models proposed here, with equivalent age-dependent parameters as described in Sect. 6. More complete model (3.2) may give more precise results, but it also requires more detailed age-specific immunological data, which may not be easily available. On the other hand, model (4.5) and the delay model (5.1) require less detailed data. As per the estimates regarding the recovery and death rates determined in Sect. 6.4, the mean values of the bimodal gamma distributions $\hat{r}(t)$ and $\hat{d}(t)$ are approximately 8

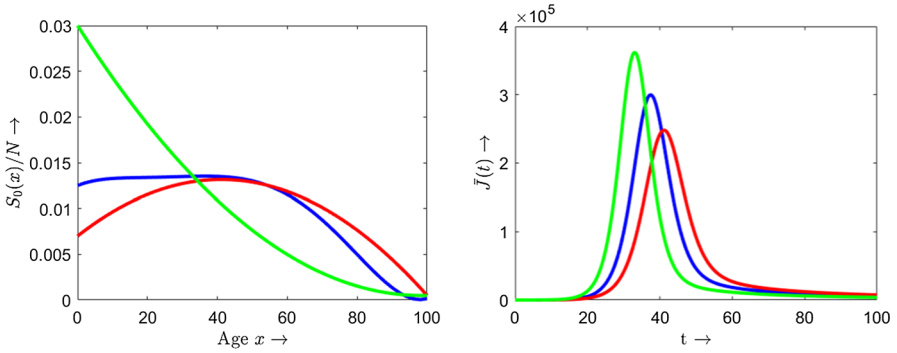

Fig. 3 **a** Different age structures $S_0(x)/N$ of the initial susceptible population with the same total population. **b** Epidemic progression for the three cases in the left panel is shown with the same color

and 20, respectively. Hence, in the delay model (5.1), we can take the age-dependent disease duration $\tau(x)$ as follows:

$$\tau(x) = 8(1 - q(x)) + 20q(x),$$

where, $q(x)$ is as estimated in Sect. 6.4. The corresponding age-dependent recovery and death rates for the model (4.5) is given by the expression

$$\gamma(x) + \delta(x) = 1/\tau(x).$$

All other parameters are the same as estimated in Sect. 6.

Numerical simulation for the three models are presented in Fig. 4. The results for the main immuno-epidemiological model (3.2) (magenta curve) coincides with the delay model (5.1) (yellow curve). However, the SIR-type model (4.5) (cyan curve) gives smaller maximal number of infected and larger time to maximum. Due to the assumption that the recovery and death rates are proportional to $I(x,t)$, this model overestimates the recovery and death rates and, consequently, underestimates the number of infected individuals.

7.3 Epidemic progression due to Omicron in New Zealand

Finally, we validate the immuno-epidemiological model (3.2) with the data on the epidemic progression in New Zealand during the Omicron outbreak. Namely, we compare modelling results with reported new daily cases from January 1, 2022 to June 25, 2022. Let us recall that new daily cases $J(x,t)$ can be expressed through the total number of infected $I(x,t)$ and the number of susceptible $S(x,t)$ (see (3.2a)). Together with the coefficients $\alpha(x)$ and $W(y)$ we can determine new daily cases $\bar{J}(t)$ for all age groups. Thus, we take $I(x,t)$ and $S(x,t)$ from the reported data, determine $J(x,t)$ by formula (3.2a), find $\bar{J}(t)$ taking a sum of all age groups and compare the result with the reported data on new daily cases.

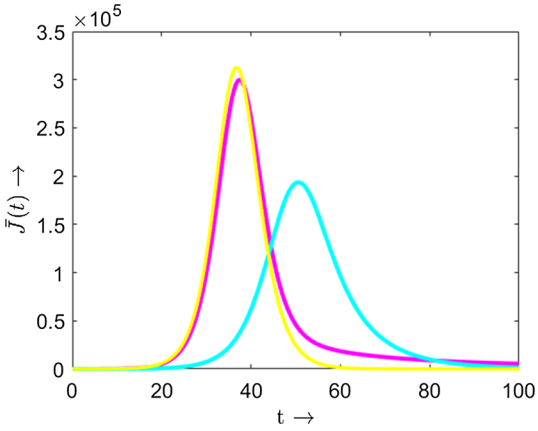

Fig. 4 The number of new daily cases in numerical simulations with the main model (3.2) (magenta curve), the model (4.5) (cyan curve) and the delay model (5.1) (yellow curve)

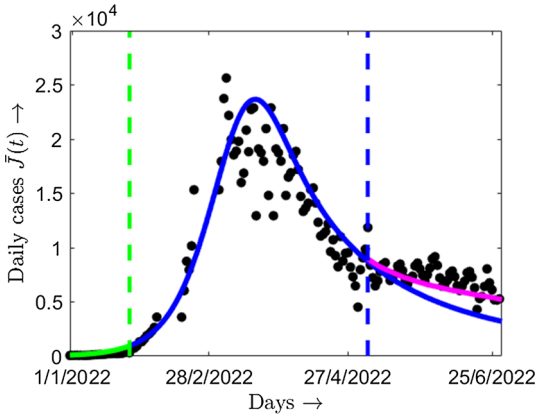

Fig. 5 Comparison of new daily cases in modelling and data: model fitting (green), model validation (blue). The black dots are the real data for Omicron in New Zealand. The magenta curve corresponds to modelling with the increased disease transmission rate due to the emergence of new strain in April, 2022

It remains to note that we determine the value of c in the expression $\alpha(x) = c\alpha_p(x)$ fitting modelling results with the data for the first 50 days (green curve in Fig. 5). We get $c = 4.4 \times 10^{-12}$.

Black dots in Fig. 5 represent the real data on daily new cases of Omicron in New Zealand, and the blue curve is the simulation result obtained as described above. We can observe that modelling results fit quite well the real data up to the end of April, 2022.

From the end of April 2022, new daily cases have some increase instead of further decreasing predicted by the model (Fig. 5). A possible explanation of this discrepancy is related to the emergence of new strain BA.2 (instead of the previous BA.1) for which vaccination can be less efficient due to immune escape or which can have a slightly larger transmission rate (Our world in data 2022). In order to describe this effect, we change the value of c from 4.4×10^{-12} to 5.7×10^{-12}, in the beginning of May, 2022. The corresponding result is shown by the magenta curve in Fig. 5, which shows a larger number of daily cases.

8 Discussion

Model with distributed parameters. Compartmental epidemiological models can be derived starting from the number of new daily cases. All other compartments, such as susceptible, infected, recovered and dead can be expressed through it with a given recovery and death rates. The latter can be taken either from the epidemiological data or considered in some simplified model form allowing, in particular, the derivation of the SIR or delay models. Previously, this approach was suggested in Ghosh et al. (2022). Here we develop it for an age-structured population.

The disease transmission rate is supposed to be proportional to the intra-individual viral load. It can be considered as a distributed function depending on time from the infection onset (Grassly and Fraser 2008), or as an average value determined by the virus replication rate and individual immune response. We use in this work the second approach since it is more appropriate for age-structured populations, and obtain the immuno-epidemiological model. Indeed, exposed individuals become infectious when the viral load in the upper respiratory tract becomes sufficiently large. In the case of COVID-19 this latent period is sufficiently short. Depending on SARS-CoV-2 variant, it can be between 2 and 5 days. The time-dependent infectivity rate is considered in our previous work Ghosh et al. (2022b), where it was taken into account through the distributed infectivity rate proportional to viral load depending on time from the infection onset. However, taking into account time-dependent and age-dependent infectivity rates at the same time leads to a more complex model. In order to avoid this excessive complexity, we neglect here the latency in the disease transmission rate. This question will be considered in the forthcoming works.

The influence of asymptomatic individuals was largely discussed in the literature devoted to COVID-19 pandemic. The estimated number of asymptomatic cases can vary between 25% and 50% (Nishiura et al. 2020; Mizumoto et al. 2020). Moreover, they can also transmit the disease (Huff and Singh 2020). Formally, they can be introduced in the model as a separate compartment with a different disease transmission rate. However, viral load and disease transmission rate are smaller for asymptomatic individuals. Therefore, infected by those individuals have a smaller initial viral load and will likely be also asymptomatic (though it depends on the individual immune response). Hence, in the first approximation, we can expect that the influence of asymptomatic on symptomatic subclass can be neglected.

SIR and delay models. The data on distributed recovery and death rates depending on time from the infection onset are not easily available, moreover, for different age groups. Therefore, some simplified models are of interest. Conventional SIR model and delay model can be obtained as two limiting cases, for constant (time-independent) recovery and death rates and for concentrated (delta-function) rates.

Comparison of these three models shows that SIR model overestimates recovery and death because they begin right after infection onset (constant rates), while this is not the case in reality. On the other hand, delay model with an average disease duration gives practically the same result as the distributed model. This conclusion allows the simplification of modelling approach since we do not need to determine

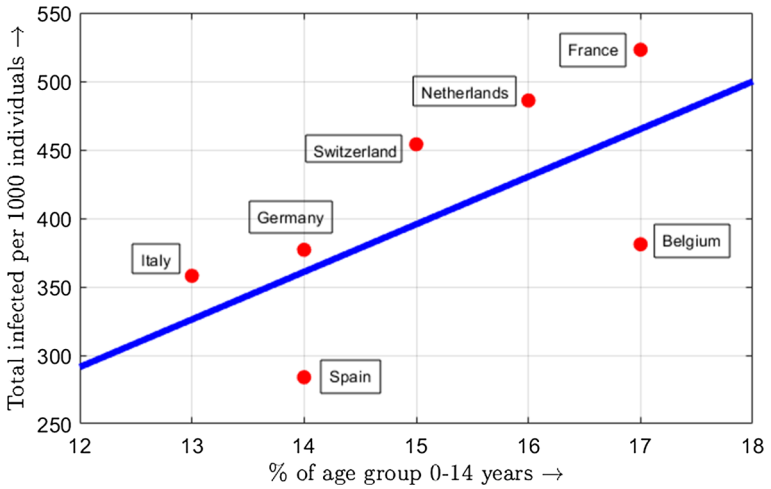

Fig. 6 Percentage of the age group 0-14 years (https://donnees.banquemondiale.org/indicator/SP.POP.0014.TO.ZS) versus the total number of infection cases from the beginning of epidemic till August 21, 2022 with respect to 1000 people (https://www.worldometers.info/coronavirus/#countries)

distributed rate functions, and the point-wise delay model is simpler than the model with distributed delay (Ghosh et al. 2022a).

Age-dependent populations. The main novelty of this work in comparison with the previous ones is that we consider age-dependent populations together with distributed recovery and death rates. We show that proportion of young age groups influences the epidemic progression since disease transmission rate is higher for them. Figure 3 clearly illustrates that if proportion of the young age groups increases (green curves), then the maximal number of newly infected individuals also increases while the time to maximum decreases due to higher infection transmission by younger population in case of Omicron (see Fig. 1b). On the other hand, for a smaller proportion of the younger age group (red curves), the maximal number of new infections decreases and the time to maximum increases in Fig. 3. Though it can be difficult to justify this conclusion with the data from different countries because of the influence of numerous other factors (climate, economy, social restrictions) and different methods of data collection, if we restrict this comparison to some neighboring European countries, for which these differences can be less essential, then some tendency can be observed (Fig. 6).

Vaccination. In this work, we do not take into account the influence of vaccination. However, during Omicron outbreak many countries (including New Zealand) reached a plateau in the number of vaccinated people. Therefore, vaccination can be taken into account implicitly through the fitted parameter c which includes the proportionality coefficient to the number of susceptible reduced due to vaccination.

This argument is applicable for the Omicron outbreak since the booster vaccine dose was fully efficient. However, in a longer time scale, immunity waning decreases vaccine efficiency and can lead to further epidemic outbreaks. Let us note that more

detailed models taking into account vaccination dynamics and vaccine waning can give reliable predictions of epidemic progression (Ghosh et al. 2022b).

Collective immunity. The question of collective immunity was largely discussed in the beginning of epidemic. However, the measures of social distancing which were necessarily introduced to decrease the number of hospitalizations and collapse of public health system, kept the number of infected individuals essentially below the level of collective immunity.

The situation was quite different during the Omicron outbreak. Relatively weak symptoms and low mortality rate did not require strong social distancing measures. They remained quite relaxed and unchanged in many countries. On the other hand, high transmission rate and decreased number of susceptible due to vaccination and disease acquired immunity allowed some countries to reach the level of collective immunity (Saldaña and Scoglio 2022). The number of daily infected passed through the maximal value and decreased due to the decrease of the susceptible population. Similar behavior is observed in the simulations presented above.

Let us note that collective immunity does not imply the end of epidemic because of the immunity waning and possible emergence of new strains. However, after two years of COVID-19 epidemic, we can expect that it approaches a long-term dynamics with some ground-based level of infected individuals and occasional outbreaks due to seasonal changes and new variants.

Limitations and perspectives. We have already mentioned above that we did not consider in this work exposed and asymptomatic cases which can possibly influence the epidemic progression up to certain extent. They can be introduced in more detailed models, but rigorous analysis of the concerned model can be quite involved. Introduction of vaccination in the model allows a longer and more reliable prediction of epidemic progression and controlling further outbreaks. Finally, let us note that the models considered in this work are generic and can be applied to other epidemics. Especially, this concerns more simple and still accurate delay model.

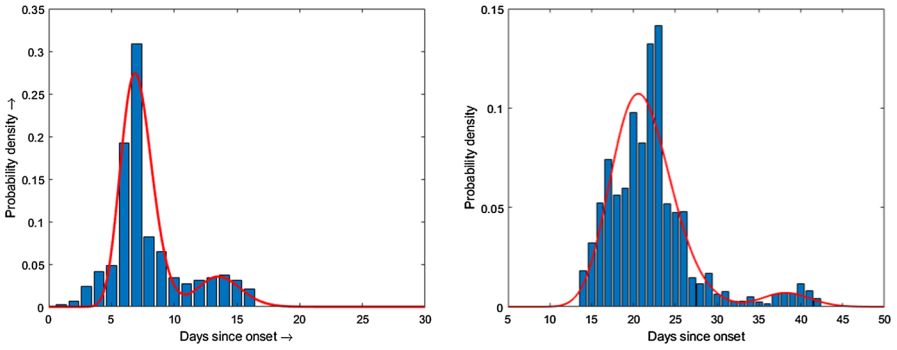

Fig. 7 Probability distribution (taken from Ghosh et al. (2022b); Sharma et al. (2022)) of (a) recovery $\hat{r}(t)$ and (b) death $\hat{d}(t)$ as functions of time (in days) after the onset of infection. The red curves show the best fitted bimodal gamma distributions

Acknowledgements The authors express their gratitude to the learned reviewers for the insightful comments and suggestions. This publication has been supported by the RUDN University Scientific Projects Grant System, Project No 025141-2-174.

Declarations

Conflict of interest The authors declare that they have no conflict of interest.

Appendix 1: Recovery and death distributions

The time dependent average recovery ($\hat{r}(t)$) and death ($\hat{d}(t)$) distributions are shown in Fig. 7.

Appendix 2: Statistical tools

Gamma distributions are estimated using the inbuilt function *fitdist(:,gamma)* in MATLAB. This function is used to fit a vector of data $X = (x_1, x_2, \ldots, x_n)$ by a gamma distribution of the form $\frac{1}{b^a \Gamma(a)} x^{a-1} e^{-x/b}$, where a and b are the shape and scale parameters. This function gives the maximum likelihood estimators of a and b for the gamma distribution which are the solutions of the simultaneous equations

$$\log \hat{a} - \Psi(\hat{a}) = \log\left(\bar{X}/\Big(\prod_{i=1}^{n} x_i\Big)^{1/n}\right),$$
$$\hat{b} = \bar{X}/\hat{a},$$

where $\bar{X}$ is the sample mean of the data X and Ψ is the digamma function given by

$$\Psi(x) = \Gamma'(x)/\Gamma(x).$$

The function *fitdist(:,gamma)* estimates the shape and scale parameters with 95% confidence interval.

All other estimations and curve fittings are done by minimizing the Sum of Squared Errors (SSE). We applied three methods to minimize the SSE function: first, gradient-based method followed by a step of minimization with a gradient-free method, again followed by a third step of gradient-based method. MATLAB nonlinear least-square solvers *fmincon* and *patternsearch* are used to fit day-wise number of cases. Detailed description of this method and its implementation can be found in Kelley (1999).

References

Wikipedia (2018) https://en.wikipedia.org/wiki/2018_New_Zealand_census#Age

Our world in data (2022) https://ourworldindata.org/grapher/covid-cases-omicron?time=2022-01-24&country=GBR~FRA~BEL~DEU~ITA~ESP~USA~ZAF~BWA~AUS

Baccam P, Beauchemin C, Macken CA, Hayden FG, Perelson AS (2006) Kinetics of influenza a virus infection in humans. J Virol 80(15):7590–7599
Bansal S, Grenfell BT, Meyers LA (2007) When individual behaviour matters: homogeneous and network models in epidemiology. J R Soc Interface 4(16):879–891
Barbarroux L, Michel P, Adimy M, Crauste F (2016) Multi-scale modeling of the cd8 immune response. In: AIP Conference Proceedings, vol 1738, p 320002. AIP Publishing LLC
Barbarroux L, Michel P, Adimy M, Crauste F (2018) A multiscale model of the cd8 t cell immune response structured by intracellular content. Discrete Contin Dyn Syst Ser B 23(9):3969
Bichara D, Iggidr A (2018) Multi-patch and multi-group epidemic models: a new framework. J Math Biol 77(1):107–134
Bocharov G, Volpert V, Ludewig B, Meyerhans A et al (2018) Mathematical immunology of virus infections. Science 245:996
Bouchnita A, Jebrane A (2020) A hybrid multi-scale model of Covid-19 transmission dynamics to assess the potential of non-pharmaceutical interventions. Chaos Solitons Fractals 138(109941):998
Brauer F (2008) Compartmental models in epidemiology. In: Mathematical epidemiology, pp 19–79. Springer
Brauer F, Castillo-Chavez C, Feng Z(2019) Mathematical models in epidemiology, vol 32. Springer
Castillo-Chavez C, Feng Z (1998) Global stability of an age-structure model for tb and its applications to optimal vaccination strategies. Math Biosci 151(2):135–154
Chattopadhyay AK, Choudhury D, Ghosh G, Kundu B, Nath SK (2021) Infection kinetics of Covid-19 and containment strategy. Sci Rep 11(1):1–12
Chen H, Smith G, Li K, Wang J, Fan X, Rayner J, Vijaykrishna D, Zhang J, Zhang L, Guo C et al (2006) Establishment of multiple sublineages of h5n1 influenza virus in asia: implications for pandemic control. Proc Natl Acad Sci 103(8):2845–2850
D'Agata EM, Magal P, Ruan S, Webb G (2006) Asymptotic behavior in nosocomial epidemic models with antibiotic resistance. Differ Integral Equ 19(5):573–600
Fenichel EP, Castillo-Chavez C, Ceddia MG, Chowell G, Parra PAG, Hickling GJ, Holloway G, Horan R, Morin B, Perrings C et al (2011) Adaptive human behavior in epidemiological models. Proc Natl Acad Sci 108(15):6306–6311
von Foerster L (1959) Some remarks on changing populations in the kinetics of cellular proliferation, pp 382–407. Grune & Stratton. [Google Scholar]
Frieden TR, Damon I, Bell BP, Kenyon T, Nichol S (2014) Ebola 2014-new challenges, new global response and responsibility. N Engl J Med 371(13):1177–1180
Gao D, Ruan S (2012) A multipatch malaria model with logistic growth populations. SIAM J Appl Math 72(3):819–841
Ghosh S, Banerjee M, Volpert V (2022) An epidemic model with time delay determined by the disease duration. Mathematics 10:2561
Ghosh S, Banerjee M, Volpert V (2022) Immuno-epidemiological model-based prediction of further Covid-19 epidemic outbreaks due to immunity waning. Math Model Nat Phenom 17:9
Ghosh S, Volpert V, Banerjee M (2022) An epidemic model with time-distributed recovery and death rates. Bull Math Biol 84(8):1–19
Gilchrist MA, Sasaki A (2002) Modeling host-parasite coevolution: a nested approach based on mechanistic models. J Theor Biol 218(3):289–308
Girard MP, Tam JS, Assossou OM, Kieny MP (2010) The 2009 a (h1n1) influenza virus pandemic: a review. Vaccine 28(31):4895–4902
Grassly NC, Fraser C (2008) Mathematical models of infectious disease transmission. Nat Rev Microbiol 6(6):477–487
Hethcote HW, Van den Driessche P (1991) Some epidemiological models with nonlinear incidence. J Math Biol 29(3):271–287
Hirotsu Y, Maejima M, Shibusawa M, Natori Y, Nagakubo Y, Hosaka K, Sueki H, Mochizuki H, Tsutsui T, Kakizaki Y et al (2022) Sars-cov-2 omicron sublineage ba. 2 replaces ba. 1.1: Genomic surveillance in japan from september 2021 to March 2022. J Infect 3:958
Huff HV, Singh A (2020) Asymptomatic transmission during the coronavirus disease 2019 pandemic and implications for public health strategies. Clin Infect Dis 71(10):2752–2756
Jansen VA, Lloyd AL (2000) Local stability analysis of spatially homogeneous solutions of multi-patch systems. J Math Biol 41(3):232–252

Kang H, Huang Q, Ruan S (2020) Periodic solutions of an age-structured epidemic model with periodic infection rate. Commun Pure Appl Anal 19(10):4955
Kang H, Ruan S (2021) Mathematical analysis on an age-structured sis epidemic model with nonlocal diffusion. J Math Biol 83(1):1–30
Kang H, Ruan S (2021) Principal spectral theory and asynchronous exponential growth for age-structured models with nonlocal diffusion of neumann type. Math Ann 5:1–49
Kelley CT (1999) Iterative methods for optimization. SIAM 3:689
Kermack WO, McKendrick AG (1927) A contribution to the mathematical theory of epidemics. Proc Math Phys Eng Sci 115(772):700–721
Kermack WO, McKendrick AG (1932) Contributions to the mathematical theory of epidemics. ii.-the problem of endemicity. Proc Math Phys Eng Sci 138(834):55–83
Kermack WO, McKendrick AG (1933) Contributions to the mathematical theory of epidemics. iii.-further studies of the problem of endemicity. Proc Math Phys Eng Sci 141(843):94–122
Kilpatrick AM, Chmura AA, Gibbons DW, Fleischer RC, Marra PP, Daszak P (2006) Predicting the global spread of h5n1 avian influenza. Proc Natl Acad Sci 103(51):19368–19373
Kuniya T (2011) Global stability analysis with a discretization approach for an age-structured multigroup sir epidemic model. Nonlinear Anal Real World Appl 12(5):2640–2655
Kuniya T, Inaba H (2013) Endemic threshold results for an age-structured sis epidemic model with periodic parameters. J Math Anal Appl 402(2):477–492
Kuniya T, Wang J, Inaba H (2016) A multi-group sir epidemic model with age structure. Discrete Contin Dyn Syst Ser B 21(10):3515
Levin AT, Hanage WP, Owusu-Boaitey N, Cochran KB, Walsh SP, Meyerowitz-Katz G (2020) Assessing the age specificity of infection fatality rates for covid-19: systematic review, meta-analysis, and public policy implications. Eur J Epidemiol 35(12):1123–1138
Li XZ, Yang J, Martcheva M (2020) Nested immuno-epidemiological models. In: Age structured epidemic modeling, pp 69–103. Springer
Lindquist J, Ma J, Van den Driessche P, Willeboordse FH (2011) Effective degree network disease models. J Math Biol 62(2):143–164
Liu Z, Chen J, Pang J, Bi P, Ruan S (2018) Modeling and analysis of a nonlinear age-structured model for tumor cell populations with quiescence. J Nonlinear Sci 28(5):1763–1791
Mizumoto K, Kagaya K, Zarebski A, Chowell G (2020) Estimating the asymptomatic proportion of coronavirus disease 2019 (covid-19) cases on board the diamond princess cruise ship, yokohama, japan, 2020. Eurosurveillance 25(10):2000180
Müller J (1998) Optimal vaccination patterns in age-structured populations. SIAM J Appl Math 59(1):222–241
Nishiura H, Kobayashi T, Miyama T, Suzuki A, Jung S, Hayashi K, Kinoshita R, Yang Y, Yuan B, Akhmetzhanov AR et al (2020) Estimation of the asymptomatic ratio of novel coronavirus infections (covid-19). Int J Infect Dis 94:154–155
Ou C, Wu J (2006) Spatial spread of rabies revisited: influence of age-dependent diffusion on nonlinear dynamics. SIAM J Appl Math 67(1):138–163
Paul S, Lorin E (2021) Estimation of Covid-19 recovery and decease periods in Canada using delay model. Sci Rep 11(1):1–15
Qesmi R, ElSaadany S, Heffernan JM, Wu J (2011) A hepatitis b and c virus model with age since infection that exhibits backward bifurcation. SIAM J Appl Math 71(4):1509–1530
Qesmi R, Heffernan JM, Wu J (2015) An immuno-epidemiological model with threshold delay: a study of the effects of multiple exposures to a pathogen. J Math Biol 70(1):343–366
Rockett RJ, Arnott A, Lam C, Sadsad R, Timms V, Gray KA, Eden JS, Chang S, Gall M, Draper J et al (2020) Revealing Covid-19 transmission in Australia by sars-cov-2 genome sequencing and agent-based modeling. Nat Med 26(9):1398–1404
Saldaña J, Scoglio C (2022) Influence of heterogeneous age-group contact patterns on critical vaccination rates for herd immunity to sars-cov-2. Sci Rep 12(1):1–12
Sharma RP, Gautam S, Sharma P, Singh R, Sharma H, Parsoya D, Deba F, Bhomia N, Potdar VA, Yadav PD et al. (2022) Clinico epidemiological profile of omicron variant of sars-cov-2 in Rajasthan. medRxiv (2022)
Shim E, Feng Z, Martcheva M, Castillo-Chavez C (2006) An age-structured epidemic model of rotavirus with vaccination. J Math Biol 53(4):719–746

Vattiatio G, Lustig A, Maclaren O, Plank MJ (2022) Modelling the dynamics of infection, waning of immunity and re-infection with the omicron variant of sars-cov-2 in Aotearoa New Zealand. Epidemics 41:100657

Webb GF, D'Agata EM, Magal P, Ruan S (2005) A model of antibiotic-resistant bacterial epidemics in hospitals. Proc Natl Acad Sci 102(37):13343–13348